Design, Chirality, and Flexibility in Nanoporous Molecule-Based Materials

D. BRADSHAW, J. B. CLARIDGE, E. J. CUSSEN, T. J. PRIOR, AND M. J. ROSSEINSKY*

Department of Chemistry, The University of Liverpool, Liverpool L69 7ZD, U.K.

Received July 6, 2004

ABSTRACT

Scientific and technological interest in porous materials with molecule-sized channels and cavities has led to an intense search for controlled chemical routes to systems with specific properties. This Account details our work on directing the assembly of open-framework structures based on molecules and investigating how the response of nanoporous examples of such materials to guests differs from classical rigid porous systems. The stabilization of chiral nanoporosity by a hierarchy of interactions that both direct and maintain a helical open-framework structure exemplifies the approach.

Introduction

Porous materials offer considerable internal surface area for separation, manipulation, and catalytic transformation of guest molecules.[1,2] This Account deals with nanoporous (often termed microporous) materials with channel dimensions of <2 nm. The pre-eminent examples of such systems are the aluminosilicate zeolites, which are widely applied due to their diverse functionality, which exploits access of guest molecules to voids of molecular dimensions. For example, ultrastabilized H-zeolite Y is used in the catalytic cracking process that produces every molecule of gasoline and sorption by Li-exchanged chabazite selectively separates oxygen and nitrogen. These oxides[3] are rigid materials that display permanent porosity (i.e., the open-framework structure persists in the absence of the species around which it grows), characterized by the observation of type I guest sorption isotherms.[4] The rigidity of the links gives rise to molecular sieving, that is, only molecules of a certain size and shape can pass through the windows and access the porosity. The regular monodisperse nature of the crystalline array of micropores is essential in this function and produces an atomic-scale specificity that distinguishes these systems from other porous materials (polymers, meso- or macroporous silicas).

It is interesting to speculate whether permanently porous materials with a greater degree of flexibility could be prepared, or whether the rigidity of the oxide-based systems is a prerequisite for crystalline microporosity. The success of zeolites in applications, combined with the attraction of studying solids in which essentially every atom is at the surface, has motivated assembly of porous materials in a predictable way. This is difficult to achieve for zeolites as the local connectivity is tetrahedral due to the bonding requirements of Si and the channel structure imposed by a complex sequence of condensation and molecular recognition events around the templating species. The concept of a *secondary building unit* (SBU), a component of the structure common to several frameworks, is powerful in rationalizing (and predicting[5]) the structures of zeolites and related materials with actual prenucleation building units identified in solution.[6] The geometries offered by multidentate ligands of variable shape binding to (possibly polynuclear) metal centers allow direct access to networks of several connectivities, not restricted to tetrahedral, in which the molecular component acts as the SBU (Figure 1). Molecule-based systems can thus adopt open-framework architectures, the channels and cavities in the structure assembling around solvent molecules, with the structural topology driven by the connectivity of each node and spacer[7,8] (Figure 2a) rather than imposed by the template (Figure 2b). The resulting structure is then controlled by the number of bonds made by the bridging ligand and the coordination number of the metal.

The synthesis of open-framework structures based on molecules offers control of pore size and chemical functionality of the internal surface — pores lined with π-electrons, organic acid/base sites, or polar groups will have differing sorption and reaction properties compared with less polarizable oxide-based materials. The mechanisms governing access to the pores may differ if specific guest−host interactions can be engineered. Control over the component molecules may lead to additional functionality over oxide-based materials. To achieve such specificity, we need to understand the fundamentals controlling assembly of molecular units into open-framework structures and the types of interactions leading to permanently porous structures. The potential advantages need to be set against the thermal and chemical stability of the oxide-based systems—the Si−O bond is one of the strongest covalent interactions known, and the use

Darren Bradshaw completed a Ph.D. in bioinorganic chemistry at the University of Sheffield in 2001 under the supervision of Prof. David E. Fenton. He is currently a postdoctoral research fellow at the University of Liverpool.

John Bleddyn Claridge obtained his B.A. and D.Phil. (1996) from the University of Oxford, he held postdoctoral positions at the University of South Carolina and the University of Oxford and has been a lecturer at the University of Liverpool since 1999.

Edmund Cussen received his B.Sc. from the University of Nottingham in 1995 and his D.Phil. from the University of Oxford in 1999. He then worked at the University of Liverpool before taking up a Royal Society University Research Fellowship at the University of Nottingham in 2002.

Tim Prior was born in Essex, U.K., in 1976 and was awarded M.Chem. and D.Phil. degrees from the University of Oxford. He is currently engaged in postdoctoral work for Professor Peter Battle in Oxford.

Matthew Rosseinsky obtained his D.Phil. in 1990 under the supervision of Professor P. Day. After 2 years as a postdoctoral researcher at Bell Laboratories with D. W. Murphy, he became lecturer in Inorganic Chemistry at the University of Oxford in 1992. In 1999, he moved to the University of Liverpool as Professor of Inorganic Chemistry.

10.1021/ar0401606 CCC: $30.25
Published on Web 01/08/2005

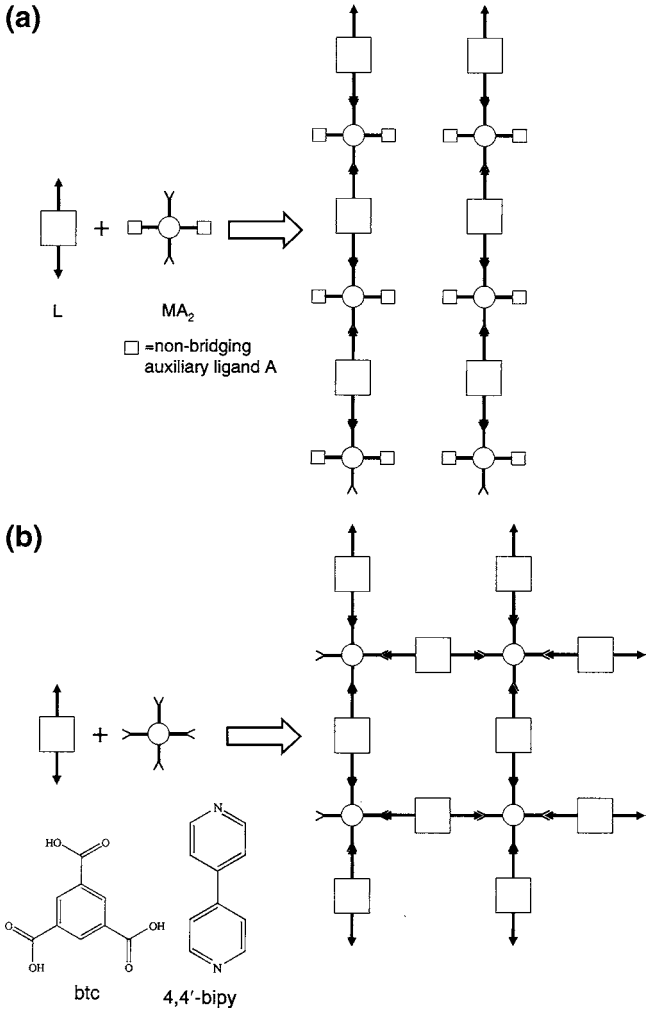

FIGURE 1. The predefined connectivities of multidentate ligands L (linear bidentate here) and metal center M allow predictable assembly of extended structures. Here M is a square planar center, which in panel a acts as a linear connector due to the coordination of two nonbridging auxiliary ligands, producing a linear chain geometry; in panel b, bidentate L coordinates all four metal sites producing a square grid array. The btc and 4,4′-bipy ligands act as three- and two-connectors, respectively.

of charged hydrated templates allows the extraframework species to play a functional role in the activated porous materials in catalysis (Figure 2d).

Synthetic strategies for the preparation of nanoporous crystalline materials may be divided into the following: (i) pH-controlled condensation of oxide units around structure-directing agents (templates). The incorporation of aliovalent defects into the framework is enabled by charged extraframework species; under aqueous conditions these are often hydrated cations and access to the porosity by removing coordinated water generates extraframework species associated with the charged sections of the framework itself. Ion-exchange can then produce catalytically active centers for Bronsted or Lewis acidity or redox catalysis. (ii) Coordination-directed assembly of metal complexes by polyfunctional organic ligands. The reduced chemical strength and mechanical stability of the bonds defining these structures makes access to truly porous systems (Figure 2c) more difficult. (iii) Partial

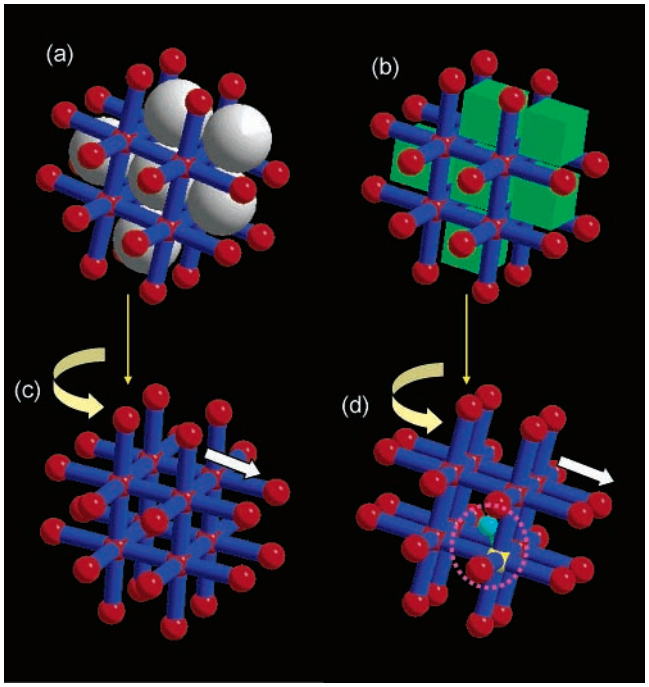

FIGURE 2. (Micro)porous materials have open-framework structures that remain stable in the absence of guests. Assembly of these structures can be programmed (a) by the directional valence of the framework constituents, represented by node (red) and spacer (blue) units wherein the material forms with guest (often solvent) species in the pores, but the guest (represented as gray spheres) does not exert a structure-directing influence or (b) by the shape, size, and charge of a templating or structure-directing agent, which constrains the geometry of the assembling structure locally. The schematic indicates how a charged template for a charged framework can be reduced in size to prepare defect sites anchored to framework charges (d). The ability to prepare such catalytically active defects is a feature of the aluminosilicate zeolites, for example, H^+ associated with framework Al^{3+} gives solid acidity. Metal-organic frameworks are prepared by guest removal (c), and the development of such defect chemistry lies in the future.

condensation of oxide components intercepted by coordination and linking by multidentate ligands.[9−11] Here the extent of oxide bridging and structure condensation increases with reaction temperature.[12] The possibilities of (ii) and (iii) to afford materials with the functionality displayed by the extended oxides from (i) are currently being explored, and it is in this context that further understanding of the link between composition, extended structure, properties, and stability is needed. This Account concerns our work with simple linking groups (trigonal 1,3,5-benzenetricarboxylate (btc) and linear 4,4′-bipyridine (bipy)) to explore this in (ii).

1. Structure Assembly—Finite and Infinite Secondary Building Units

The control exerted by the connectivity of a molecular unit over the extended structure has been documented with "default" structure types resulting from particular connectivities.[8] If the resulting array is not three-dimensional, then it can itself be an *infinite* SBU for assembly into a three-dimensional structure via a suitable linker. The

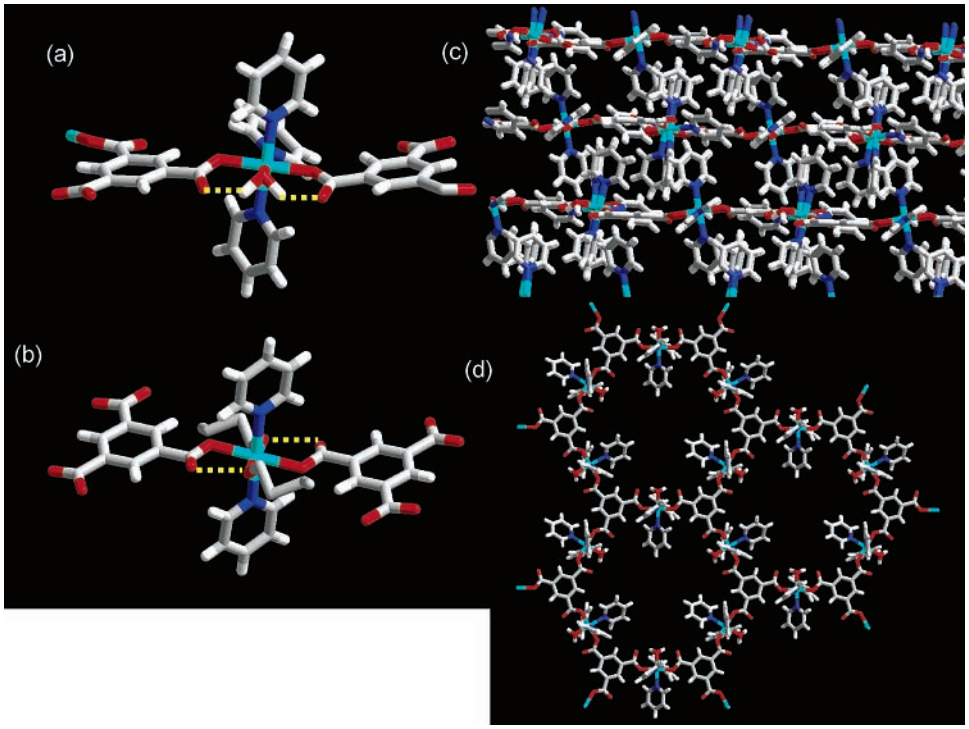

FIGURE 3. In panel a, the btc^{3-} anion planes in $Ni_3btc_2(py)_9(H_2O)_3$ are coplanar due to hydrogen bonding (broken yellow line) to the water molecule bound to Ni. In panel b, in $Ni_3btc_2(py)_6(n\text{-}C_4H_9OH)_6$, the two trans butanol molecules play a similar role to the water molecule in panel a in orienting the planes of the btc anions: here the different ligand geometry places the carboxylate groups on opposite sides of the metal with resultant puckering of the layers. Panel c shows the ABC stacking of the honeycomb (6,3) layers in panel a. In panel d, the planar (6,3) sheet has voids at the center of each 48-atom ring.

chemistry of btc^{3-} with Ni^{2+} is dominated by trans diaxial coordination of carboxylate groups to an octahedral metal center. The dimensionality of the resulting three-connected structure is controlled by hydrogen-bonding interactions between the nonbonding oxygens of the two trans btc carboxylates and the remaining auxiliary (nonframework forming) ligands at the metal. An auxiliary ligand set of three pyridines and one water molecule results in two hydrogen bonds being formed to the carbonyls, which are in the same plane, thereby producing a flat three-connected network with a honeycomb structure, known as the (6,3) net ((*n*,*m*) describe an *m*-connected net in which *n*-nodes described the shortest closed loop within the net)[13] (Figure 3).

These (6,3) structures all contain pyridine ligands projecting perpendicular to the layers. The ABC stacking occludes most of the potential void volume offered by an AAA stacking of the layers with hexagonal pores (Figure 3c,d). Clearly if the layers can be eclipsed and separated, the resulting material will have extensive extraframework volume generated from the infinite (6,3) net building units. We have covalently linked the layers by using bidentate nitrogen ligands to connect metal centers by substitution for two axial monodentate pyridines. The directionality of the bonding at the connecting ligand exerts a strong effect on the layer geometry. 4-Amino pyridine (4-AP) usually functions as a monodentate ligand via its pyridine function but is able to bridge two layers by also employing the primary amino group[14] (Figure 4a). The angle between the lone pairs (Figure 4b) renders the layers completely nonplanar (Figure 4c). The Ni_3btc_2 layer retains the (6,3) connectivity but now consists of a chair conformation of hexagons. The puckered sheet geometry is thus reminiscent of $(CF)_x$ and contrasts with the graphitic structure of the infinite SBU. Although the 4-AP ligands connect Ni atoms between layers, they do not link crystallographically equivalent Ni sites (Figure 4a), thus preventing the alignment of the pore centers in Figure 3d, so the desired linking of rigid parallel sheets is not achieved.

The 4,4′-bipyridyl ligand is a truly linear connector, and reaction with Ni^{2+} and btc^{3-} in ethylene glycol (eg) allows linkage of planar (6,3) nets[15] stacked in an AAA manner (Figure 5a) to generate channels both parallel (12.3 Å diameter, Figure 5b) and perpendicular (8 Å × 4.4 Å, Figure 5c) to the stacking direction, with large voids (13.5 Å diameter) at their intersection; the void volume is 74% of the total.

2. Permanent Porosity in Flexible and Guest-Responsive Materials

The classical view of microporous materials (zeolites, carbon molecular sieves) associates the stability of the permanent porosity with the structural rigidity conferred by strong Si−O or C−C bonds. Because the coordinate-bond-based materials cannot compete with zeolites on the basis of stability, it is reasonable to focus attention on qualitatively new behavior of the molecule-based systems. In comparison of the structures of these systems with microporous materials where the nodes are atoms,

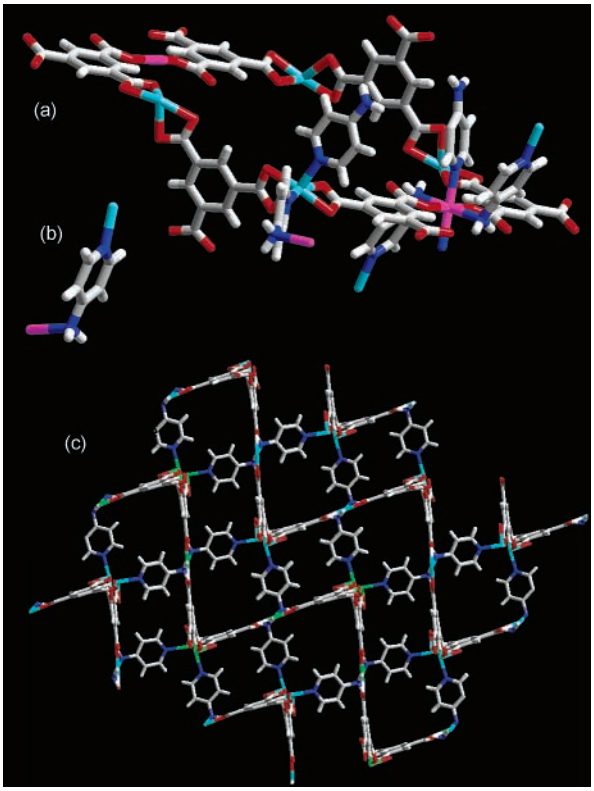

FIGURE 4. In panel a, the btc anions within each hexagon of metal atoms in the 4-AP-bridged Ni_3btc_2 phase adopt a "chair" conformation while maintaining the (6,3) topology. There are two metal sites: those rendered in purple bind to the primary amine of the bridging 4AP and thus connect to the sites rendered in cyan via the pyridine nitrogen. Octahedral coordination at the purple sites is completed by two monodentate 4-AP ligands. The cyan Ni sites within the hexagon are coordinated via a bidentate 4-AP to purple sites in adjacent layers. 4-AP ligands are only shown at two of the six sites for clarity. In panel b, the bidentate 4-AP ligand is a nonlinear connector of the two Ni sites. In panel c, the cross-linking of the puckered (6,3) layers by 4-AP produces a 113.4° angle subtended at the primary amino nitrogen by the two connected Ni atoms. The Ni atoms within one (6,3) unit are represented in green to emphasize the loss of planarity.

the internal degrees of freedom (rotation, torsion, vibration) of the molecular units become apparent. Detailed isotherm measurements reveal that these materials can display sorption behavior that is qualitatively distinct from that of the rigid classical materials[16,17] while meeting the criteria of permanent porosity. To demonstrate this, we consider two simple materials that are polymorphs of composition $Ni_2(bipy)_3(NO_3)_4$.[18−22] The frameworks are formed by T-shaped coordination of bipy to Ni^{2+} with nitrate counterions, which complete pseudo-square pyramidal coordination at the metal (Figure 6). The polymorph formed with methanol guests adopts the "ladder" structure **A**. The material is thermally stable to 175 °C and displays type I sorption isotherms. This occurs despite the 1D nature of the extended coordinate bond network, the thermal robustness arising from a network of unconventional C−H···O hydrogen bonds (Figure 6g). The combination of flexibility and robustness that this hierarchy of stability-conferring bonds gives to the network is the key to its unusual guest response. The porosity consists of cavities at the centers of the ladders interconnected by much smaller windows (2.5 Å × 4.9 Å). The material is however able to reversibly sorb toluene, which has smallest dimensions 4 Å × 6.6 Å, that is, a 26 Å^2 cross-section molecule can pass through a 12.5 Å^2 window (Figure 7). This behavior is driven by the availability of a suitable site for the guest toluene molecule in the cavity but is quite the opposite of what would be expected for a rigid porous material—guest sorption in this flexible material is controlled by the size of cavities rather than the size of the windows. For sorption to be observed, the guest must be able to drive opening of the windows in the structure giving access to the porosity, forcing the framework to open up to allow access to the cavity where modeling indicates that the guest interacts with the framework by π-stacking interactions. It is important to note that guest uptake occurs even at the lowest vapor pressures with a type I response to toluene vapor, suggesting a low barrier to window opening via torsional motion of the bipy units forming the windows. The solid thus responds directly to the presence of the guest. In large biomolecules, substrates gain access to active sites by forcing opening of the structure, and the response of the thermally robust microporous $Ni_2(bipy)_3(NO_3)_4$ framework is more reminiscent of this than of the rigid response of a zeolite. As in biological systems, the guest−framework interaction energy is comparable to that required for network deformation, the higher deformation energies for oxides disfavoring a similar flexibility of response. In the flexible systems, the acceptable guest size is controlled by the cavity rather than the window dimensions: for **A**, xylenes are sorbed but 1,3,5-triethylbenzene is rejected.

The role of the guest in these flexible structures is not limited to driving opening and closing of the windows. The $Ni_2(bipy)_3(NO_3)_4$ composition has an alternative polymorph **B**, grown from ethanol, in which the two infinite chains linked by the axial bipy ligand are perpendicular rather than parallel (Figure 6f). Sorption of methanol vapor into this microporous host is possible to generate a metastable material, that is, containing CH_3OH guests in a structure that is not formed by direct reaction of the components with CH_3OH. Exposure of **B** to CH_3OH vapor results in a transition to the ladder structure **A** in which crystal habit is preserved; the requirement for the presence of liquid rather than the transition simply occurring after sorption indicates that surface nucleation by dissolution and recrystallization is required, but once this has occurred the transition propagates throughout the solid.[21] Given the close relationship between the two structure types, possible mechanisms for interconversion involving minimal bond breakage can be proposed (Figure 8). The guest-driven transformation relies on the lability and reversibility of coordinate bond formation and opens up the possibility of forming new structures inaccessible by direct reaction.

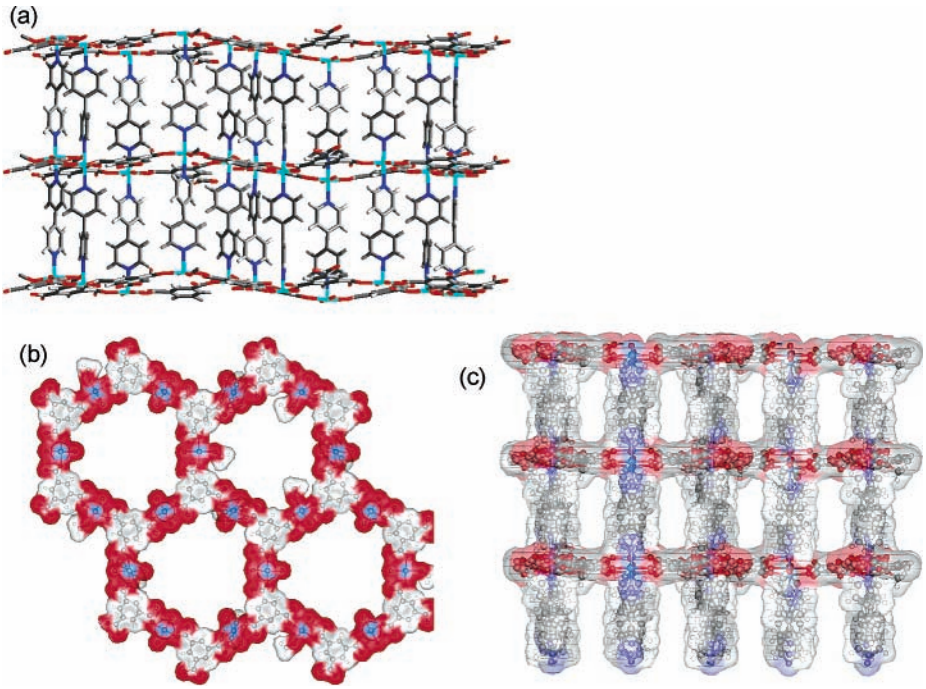

FIGURE 5. The 4,4′-bipy ligand connects two (6,3) nets in an AAA sequence (a), giving rise to channels that are (b) parallel and (c) perpendicular to the stacking direction, represented by the van der Waals surface of the framework atoms.

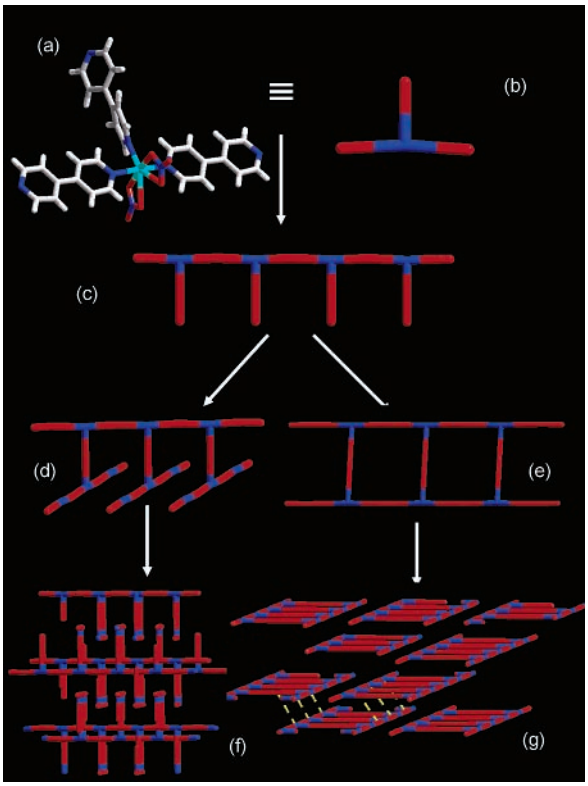

FIGURE 6. The coordination of the Ni site in both $Ni_2(bipy)_3(NO_3)_4$ polymorphs of three bipy and two nitrate groups (a) produces a "T" -shaped node (b) (Ni blue, bipy red) that produces a one-dimensional chain (c). These chains are assembled by linking via the "cross" of the T either parallel (e,g) to give one-dimensional ladders (**A**) or perpendicular (d,f) to give interlocking two-dimensional bilayers (**B**). The nonclassical C−H···O interactions responsible for the thermal stability of **A** are shown as broken yellow lines in panel g.

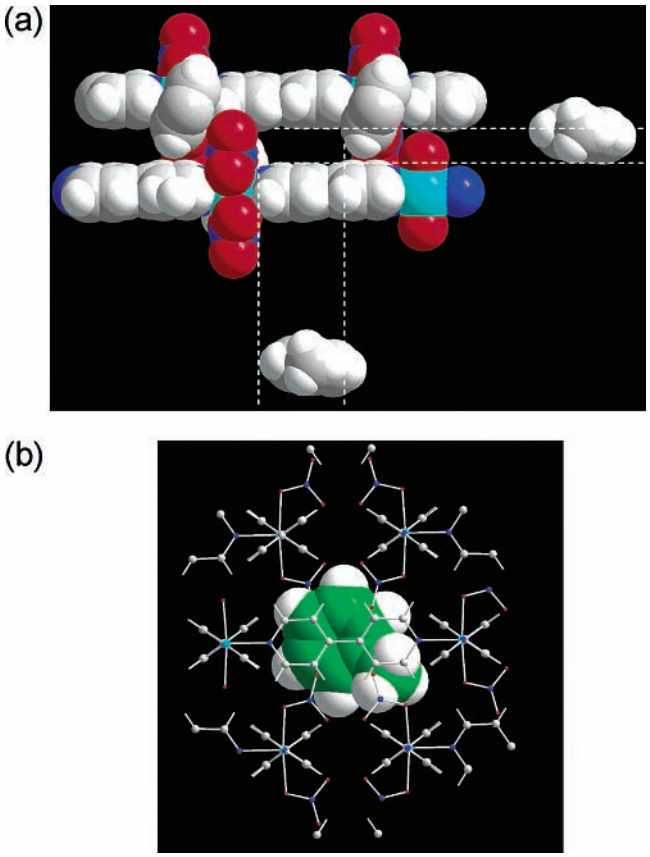

FIGURE 7. The toluene molecule is sorbed by $Ni_2(bipy)_3(NO_3)_4$ **A** because the window (a) opens to twice its resting cross-sectional area in the presence of the guest, permitting access to the cavities. In panel b, the location of toluene in the cavity is determined by Monte Carlo docking.

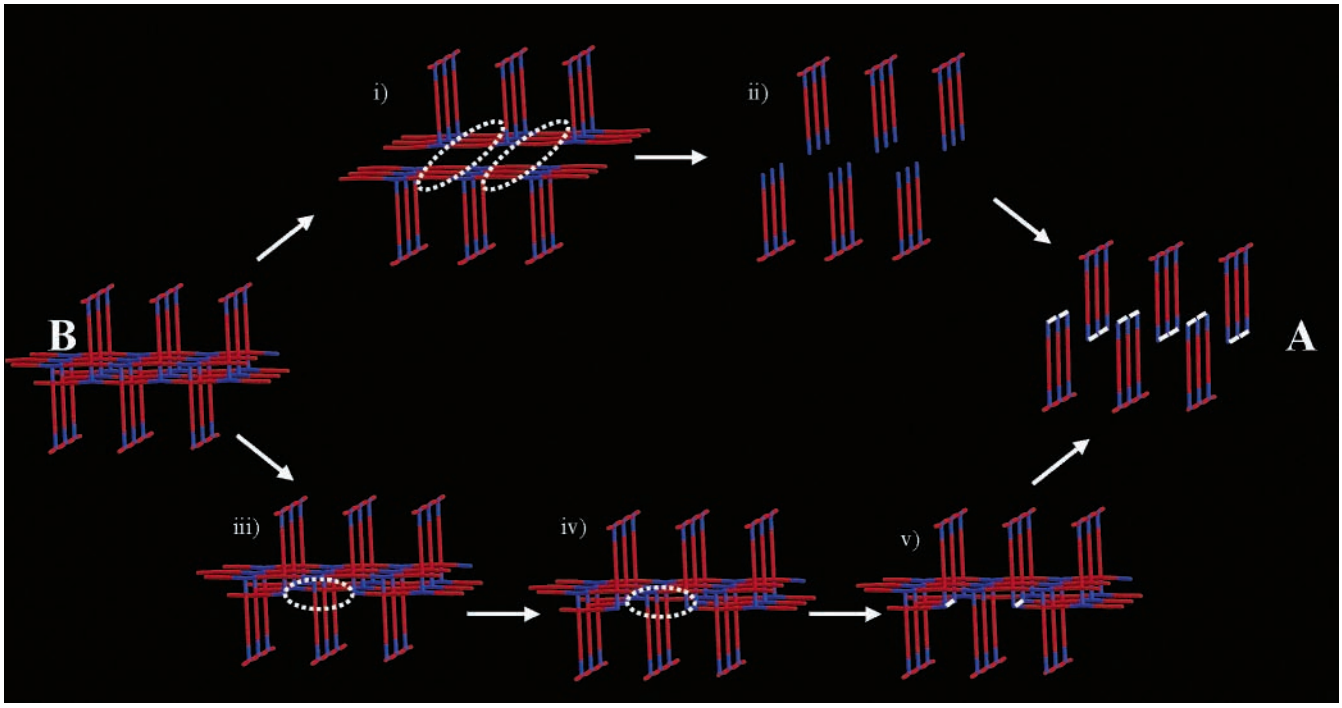

FIGURE 8. Transformation from the **B** to the **A** structure of $Ni_2(bipy)_3(NO_3)_4$ is possible via (i) separation of the bilayers, (ii) breaking $^1/_3$ of the Ni—N bonds, or (iii) breaking both Ni—N bonds at two parallel bipy molecules then rotating the Ni—N bond direction of both by 90° (v) to form a ladder defect of **A** within **B**.

3. Design and Stabilization of Permanent Microporosity in Chiral Open-Framework Materials

Chiral open frameworks are an area where it has proved demanding to confer the necessary functionality on classical nanoporous materials. Direct incorporation of chiral catalytic centers into zeolites allows enantioselective synthesis,[23] but the templating of chiral zeolite topologies is difficult because of the long distance over which chirality is expressed.[24] The use of chiral framework-forming ligands allows the generation of molecule-based open-framework structures with built-in chirality,[25] although combining this with crystallinity and permanent microporosity has thus far not proved possible. There are several noteable examples of the successful application of this strategy[26−28] Polycarboxylic amino acids are attractive building blocks for infinite chiral structures,[29,30] while the solvothermal synthesis of a porous glutarate with a chiral topology may open the way to thermally stable materials if chiral templating can be effected.[31]

One of the attractions of the molecule-based route to infinite frameworks is that there is no restriction to four-connected topologies. The ability to access three-connected networks is important because the "default"[8] three-connected three-dimensional network (i.e., the one produced unless other functionality is introduced into the building blocks to specifically favor competing structures) is the (10,3)-a net, which is chiral because it is helical[32] (Figure 9). If all the (10,3)-a nets in one crystal have the same hand, a chiral system in which the components making up the infinitely extended structure are achiral is prepared. To generate bulk chirality, the two possible helix hands must be differentiated. This can be achieved via chiral auxiliary ligands coordinated at the metal center. The search for control over the assembly of chiral structures, the stabilization of microporosity and the imposition of specific chirality has required the understanding of coordinate and nonbonded interactions in $Ni_3btc_2(ROH)_6(ArN)_6$ systems containing the three-connecting btc^{3-} anion and two auxiliary ligands (aromatic amine, ArN, alcohol, ROH).

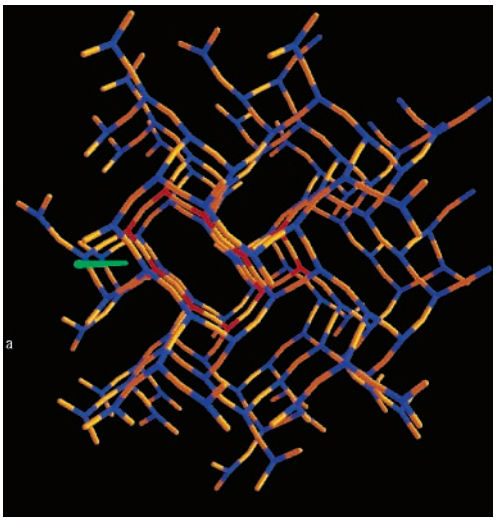

FIGURE 9. The (10,3)-a net viewed along the direction of the 4-fold helices (one is marked with a green rod). The nodes constituting a closed ten-membered loop are marked in red.

Forming the (10,3)-a Network. To generate a three-dimensional three-connected structure, coplanarity of two btc ligands bound to a metal center leading to the (6,3)

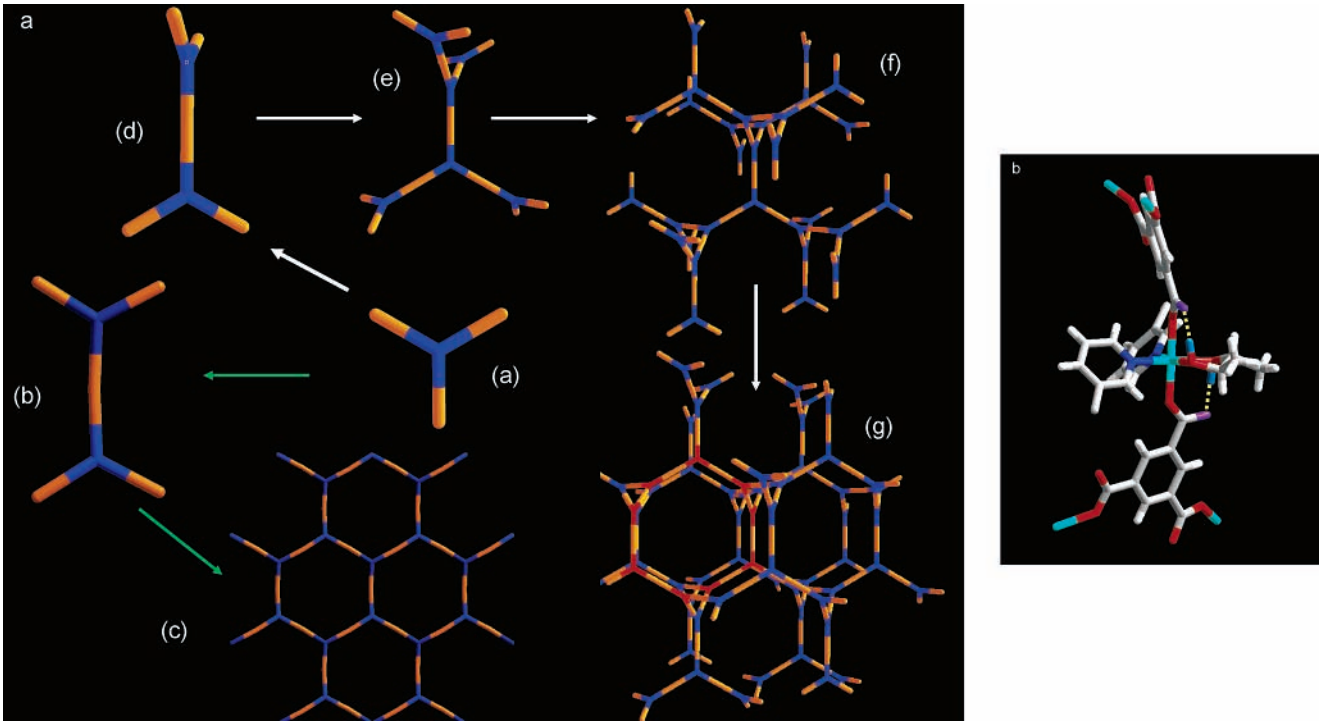

FIGURE 10. In panel a, the assembly of the two-dimensional (6,3) (green arrows) and three-dimensional (10,3)-a (white arrows) M_3btc_2 nets from the trigonal btc connector (blue, structure a) via linear M connectors (gold) is controlled by the relative orientation of the groups bound to two neighboring btc nodes. Structures b and c show how coplanarity yields the (6,3) net. In structure d, the torsional angle is 109° and propagation of this through first (structure e), second (structure f), and fifth shells (structure g) leads to the (10,3)-a net with a closed 10-node loop containing the original node shown in red. In panel b, the OH protons of the cis alcohols bound to the metal in $Ni_3btc_2(ROH)_6(ArN)_6$ structures adopting the (10,3)-a net form hydrogen bonds with the nonbonding oxygen of the btc carboxylate group, imposing a 98° torsional angle between the groups marked in purple and imposing the three-dimensional helical structure.

sheet needs to be avoided (Figure 10a). This can be achieved using hydrogen bonding within the metal coordination sphere. With trans btc carboxylates, cis location of the two alcohol ligands generates hydrogen bonding interactions involving the nonbonding oxygen from the carboxylates and the alcohol protons (Figure 10b). Because the alcohols are perpendicular to each other, the hydrogen bonding twists the two trans btc units away from coplanarity and favors the three-dimensional (10,3)-a over the two-dimensional (6,3) net. Using eg as the monodentate alcohol affords a material in which 4 (10,3)-a nets interpenetrate with the **same** handedness (Figure 11a). This 4 × (10,3)-a structure has only 26% solvent-accessible volume, although it retains crystallinity upon loss of guests at 150 °C.[33]

The auxiliary ligands in the equatorial plane of the metal center strongly control the adopted structure. Replacement of eg with 1,2-propandiol (1,2-pd) results in a *single bidentate* alcohol occupying the two oxygen coordination sites. This has a dramatic effect on the pore volume because only two rather than four networks interpenetrate, giving 51% extraframework volume (Figure 11b). As in the 4 × (10,3)-a structure, the two nets in the 2 × (10,3)-a structure have the same handedness.

Chiral Control of the 2 × (10,3)-a Structure. The difference from the 4 × (10,3)-a eg case is that 1,2-pd is itself chiral and thus can exert a chiral templating effect whereby the handedness of the small molecules coordinated to the metal centers controls the handedness of the extended helical structure. It turns out that the templating is extremely strict. In 16 crystal structures, the (*S*)-configuration of the diol gives the anticlockwise helix sense to the network, whereas the (*R*)-diol imposes clockwise helices. The origin of the templating is that the observed (*S*)-diol−anticlockwise helix and unobserved (*R*)-diol−anticlockwise helix combinations are diastereoisomers, and the nonbonded CH_3−carboxyl O contacts are beneath acceptable values in the disfavored pair (Figure 12). This selectivity is observed in crystals grown from racemic diol mixtures and allows bulk samples of one defined helix hand to be grown from resolved alcohols.

Network Stability. The stabilities of the two possible chiral structures can be strongly influenced by the aromatic amine bound to the metal center, in particular by replacing H atoms at specific points on the ring with methyl groups. 4-Picoline (4-methylpyridine) yields the 4 × (10,3)-a structure with 1,2-pd as the alcohol component, enforcing monodentate binding on the alcohol via the primary hydroxyl. The enforced removal of the chiral center from the framework reduces the correlation between helix handedness and diol stereochemistry, with a 60:40 ratio of the two enantiomers bound to the metal observed.[34]

The dense packing of the interpenetrating (10,3)-a nets in the four-net structure allows longer diol units such as 1,4-butanediol (1,4-bd) bound to the metal centers to

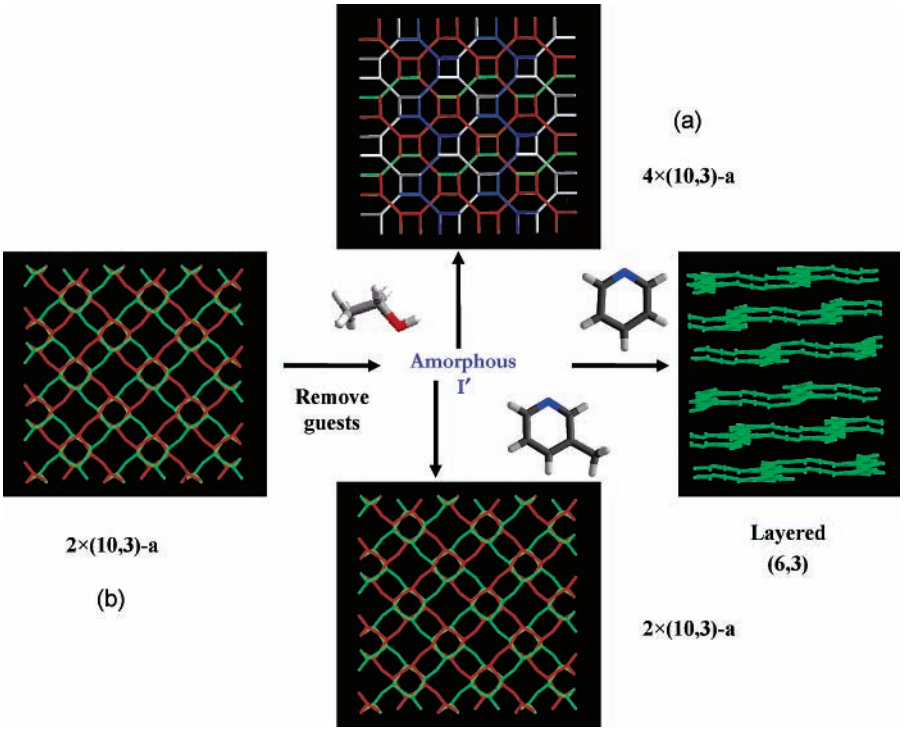

FIGURE 11. Interpenetration of four (a) and two (b) (10,3)-a networks gives rise to the Ni_3btc_2 structures found with eg and 1,2-pd, respectively, bound to the metal. Removal of guests from structure b with pyridine as auxiliary ligand leads to collapse and the formation of an amorphous, nonporous intermediate. Reaction of this intermediate with ethanol generates structure a and with pyridine the ABC stacked layered (6,3) net, whereas 3-picoline regenerates the two net phase (b).

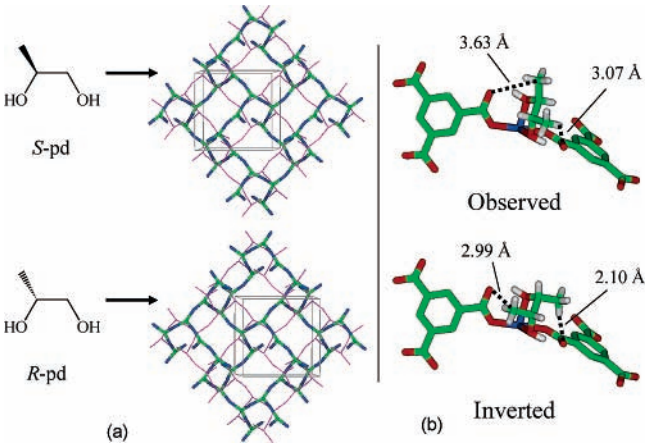

FIGURE 12. The hand of the diol bound to the metal controls the sense of all the helices within the (10,3)-a structure (a), anticlockwise with (*S*) and clockwise with (*R*) diol. In panel b, the incorrect ("inverted") combination of helix sense and diol produces less favorable nonbonded contacts between the auxiliary and framework-forming ligands.

connect two neighboring networks via coordination to metal centers.[34] One-fifth of the 1,4-butanediol ligands in $Ni_3btc_2py_6(1,4\text{-bd})_4(\mu\text{-}1,4\text{-bd})\cdot 2(1,4\text{-bd})$ link the networks to give two sets of cross linked pairs of networks. The material remains highly crystalline to 140 °C when pore solvent is lost, and the bridging 1,4-bd is retained to 200 °C.

The most interesting structure to stabilize is the 2 × (10,3)-a material, because it has a larger extraframework volume and can be chirally templated. Examination of the total composition of single crystals of this material by chiral GC shows that the helical framework is capable of recognizing the chiral 1,2-pd molecule around which it crystallizes: an 18.7% enantiomeric excess is observed, attributed to totally enantioselective coordination of 1,2-pd to the metal responsible for the chiral templating and of 1,2-pd hydrogen-bonded to the carboxylate units with the other enantiomer located at the cavity center.[33] The parent pyridine/1,2-pd material does *not* retain porosity when the guest molecules are removed from the structure and *cannot* therefore be classified as microporous. It becomes amorphous above 130 °C where guests are lost, having a BET surface area of 12 $m^2\ g^{-1}$.

These examples indicate the difficulty of predicting whether small modifications to auxiliary ligands will result in the desired structure. A useful way of discovering ligands that will stabilize specific structures is to utilize the lability of metal−organic frameworks in the presence of groups that coordinate to the metal. Although the amorphous material produced from the 1,2-pd/pyridine phase upon guest loss is nonporous, it *is* reactive to small molecules that coordinate to the metal center (Figure 11). Reaction with ethanol leads to formation of the 4 × (10,3)-a phase. Exposure to pyridine leads to the layered (6,3) phase with three pyridine molecules coordinated to the metal center. In strong contrast with pyridine, 3-picoline (3-methyl pyridine) affords the 2 × (10,3)-a chiral phase.[35] This suggests that there are specific interactions stabilizing the chiral helical structure when 3-picoline is coordinated to the metal. It is possible that these interactions will enhance the stability of the chiral phase. This

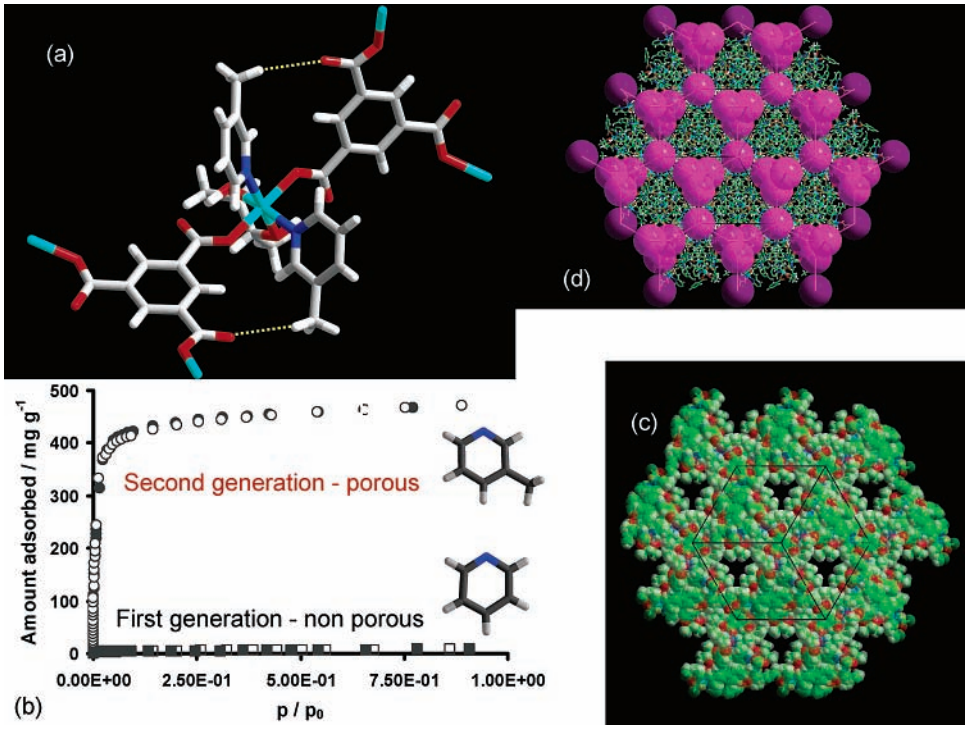

FIGURE 13. In panel a, the sole structural difference between the 3-picoline and pyridine 2 × (10,3)-a frameworks is the two C−H···O nonclassical hydrogen bonds (broken yellow line) between the carbonyl and 3-methyl groups. Isotherm data in panel b show that this is sufficient to stabilize a microporous structure in the 3-picoline case, whereas the pyridine material collapses upon removal of the guests. Panel c shows a space-filling representation of the framework with panel d representing the cavities and interconnecting channels (purple) that constitute the chiral porosity of the material, which is a (10,3)-a topology object. In panels c and d, the structure is viewed along the 111 direction.

reactive selection method of evolving structures in the presence of small molecules has the advantage over crystallization methods that solid products characterizable by powder diffraction result directly: it is also possible that the extended connectivity of framework-forming ligand to metal is present, favoring extended structures. Because many open-framework structures collapse upon loss either of solvent guests from the porosity or of auxiliary ligands bound to the metal, this reactive selection of stable frameworks by small molecule-driven crystallization of amorphous "apohosts" deserves further investigation.

The stabilization of the 2 × (10,3)-a net by 3-picoline is demonstrated by contrasting the outcome of assembly of Ni^{2+} and btc^{3-} with 1-butanol in the presence of pyridine and 3-picoline. Pyridine affords the (6,3) net with two trans pyridine and two trans alcohol auxiliary ligands. 3-Picoline produces cis auxiliary ligands and the formation of the 2 × (10,3)-a structure with a *monodentate* alcohol ligand for the first time. Comparison of the crystal structures of 1,2-pd phases with pyridine and 3-picoline reveals only one structural difference, a short distance between the proton of the extra methyl group in the 3-picoline case and the nonbonding oxygen of the btc carboxylate (Figure 13a). This interaction is also present in the 3-picoline/1-butanol material, and it is reasonable to suppose that this nonclassical hydrogen bond is the underlying factor favoring the (10,3)-a net for 3-picoline.

Loss of the guests from the 3-picoline/1,2-pd phase does *not* produce structural collapse: an isostructural guest-free cubic material with equivalent crystallinity is seen by powder diffraction, and N_2 sorption shows that a truly microporous chiral system displaying a type I isotherm (BET surface area 930 $m^2\ g^{-1}$) has been prepared[35] (Figure 13b). This confirms that the extra methyl group of the 3-picoline leads not only to selection of the chiral phase from competing structures, but also to the stabilization of that structure in the absence of guests. This is emphasized by the stability of a desolvated crystal of the 3-picoline framework: here the C−H···O interaction becomes shorter and closer to linearity, indicating that it is strengthened upon guest loss, consistent with its role in stabilizing the chiral microporosity. Probe molecules with sizes of up to 10.5 Å are kinetically rapidly sorbed in 70% of the total pore volume, showing that the majority of the porosity is accessible to large guests. The pore structure is complex (Figure 13c) and itself has the (10,3) topology with a narrowest point of 8.5 Å. However the channels are defined by conformationally flexible methyl groups forming part of a five-membered ring bound to Ni, and considering contacts to the carbon atom bearing the methyl group, an estimate of 12 Å for the narrowest point of the channels is reasonable. There are larger cavities of 13.6 Å diameter at the channel intersections (Figure 13d). Although these dimensions are larger than those found in zeolites, they work against effective discrimination between the enantiomers of small chiral molecules. Only binaphthol with dimensions 9 Å × 9 Å is enantioselectively sorbed and only with 8% ee; smaller guests such as ethyl 3-hydroxybutyrate and fenchone show

no enantioselection. This suggests that the precise matching of channel size and shape to the guest is required to prevent the relaxation of the inherently flexible framework around both enantiomers.

Conclusion

The btc-based structures show how building units and extended structures are directly related in extended molecule-based materials. The outcome of a chiral microporous material arose from the *primary* (three-connecting btc node) and *secondary* (cis location of classical hydrogen bonding groups in the metal coordination sphere) chemical bonding features to produce the required structure with the desired property of porosity conferred by the *tertiary* structural feature of a nonclassical hydrogen bond. This hierarchy of interactions could only be imposed because of the tunability of the structure, in turn resulting from the molecular nature of the constituents. The intrinsic flexibility of the material however prevented effective chiral recognition of any but the largest guests. The family of btc-based materials thus illustrate both the advantages and disadvantages of the molecule-based approach to open-framework materials.

References

(1) Davis, M. E. Ordered porous materials for emerging applications. *Nature* **2002**, *417*, 813−821.

(2) Kitagawa, S.; Kitaura, R.; Noro, S. Functional Porous Coordination Polymers. *Angew. Chem., Int. Ed.* **2004**, *43*, 2334−2375.

(3) Cheetham, A. K.; Ferey, G.; Loiseau, T. Open-framework inorganic materials. *Angew. Chem., Int. Ed.* **1999**, *38*, 3268−3292.

(4) Rouquerol, J.; Avnir, D.; Fairbridge, C. W.; Everett, D. H.; Haynes, J. H.; Pericone, N.; Ramsay, J. D. F.; Sing, K. S. W.; Unger, K. K. Recommendations for the characterisation of porous solids. *Pure Appl. Chem.* **1994**, *66*, 1739−1758.

(5) Mellot-Draznieks, C.; Girard, S.; Ferey, G. Novel inorganic frameworks constructured from double-four-ring units: Computational design, structures, and lattice energies of silicate, aluminophosphate, and gallophosphate candidates. *J. Am. Chem. Soc.* **2002**, *124*, 15326−15335.

(6) Taulelle, F. Crystallogenesis of microporous metallophosphates. *Curr. Opin. Solid-State Mater. Sci.* **2001**, *5*, 397−405.

(7) Hoskins, B. F.; Robson, R. Infinite polymeric frameworks consisting of three dimensionally linked rod-like segments. *J. Am. Chem. Soc.* **1989**, *111*, 5962−5964.

(8) Yaghi, O.; O'Keeffe, M.; Ockwig, N.; Chae, H.; Eddaoudi, M.; Kim, J. Reticular synthesis and the design of new materials. *Nature* **2003**, *423*, 705−714.

(9) Forster, P. M.; Cheetham, A. K. Open-framework nickel succinate, $[Ni_7(C_4H_4O_4)_6(OH)_2(H_2O)_2]\ {}_2H_2O$: A new hybrid material with three-dimensional Ni−O−Ni connectivity. *Angew. Chem., Int. Ed.* **2002**, *41*, 457−459.

(10) Hagrman, P. J.; Finn, R. C.; Zubieta, J. Molecular manipulation of solid-state structure: influences of organic components on vanadium oxide architectures. *Solid State Sci.* **2001**, *3*, 745−774.

(11) Zheng, L. M.; Whitfield, T.; Wang, X.; Jacobson, A. J. Hybrid Coordination Polymers − Metal Oxide Compounds with Chiral Structures. *Angew. Chem., Int. Ed.* **2000**, *39*, 4528−4531.

(12) Forster, P. M.; Burbank, A. R.; Livage, C.; Ferey, G.; Cheetham, A. K. The role of temperature in the synthesis of hybrid inorganic−organic materials: the example of cobalt succinates. *Chem. Commun.* **2004**, 368−369.

(13) Kepert, C. J.; Prior, T. J.; Rosseinsky, M. J. Hydrogen bond-directed hexagonal frameworks based on coordinated 1,3,5-benzenetricarboxylate. *J. Solid State Chem.* **2000**, *152*, 261−270.

(14) Prior, T. J.; Rosseinsky, M. J. Crystal engineering of a 3-D coordination polymer from 2-D building blocks. *Chem. Commun.* **2001**, 495−496.

(15) Prior, T. J.; Bradshaw, D.; Teat, S. J.; Rosseinsky, M. J. Designed layer assembly: a three-dimensional framework with 74% extra-framework volume by connection of infinite two-dimensional sheets. *Chem. Commun.* **2003**, 500−501.

(16) Fletcher, A. J.; Cussen, E. J.; Prior, T. J.; Rosseinsky, M. J.; Kepert, C. J.; Thomas, K. M. Adsorption dynamics of gases and vapors on the nanoporous metal organic framework material Ni_{-2}(4,4′-bipyridine)$_3(NO_3)_4$: Guest modification of host sorption behavior. *J. Am. Chem. Soc.* **2001**, *123*, 10001−10011.

(17) Fletcher, A. J.; Cussen, E. J.; Bradshaw, D.; Rosseinsky, M. J.; Thomas, K. M. Adsorption of gases and vapors on nanoporous Ni_2(4,4′-bipyridine)$_3(NO_3)_4$ metal-organic framework materials templated with methanol and ethanol: Structural effects in adsorption kinetics. *J. Am. Chem. Soc* **2004**, *126*, 9750−9759.

(18) Kondo, M.; Yoshitomi, T.; Seki, K.; Matsuzaka, H.; Kitagawa, S. Three-dimensional framework with channeling cavities for small molecules. *Angew. Chem., Int. Ed.* **1998**, *36*, 1725−1727.

(19) Power, K. N.; Hennigar, T. L.; Zarowotko, M. J. Crystal structure of the coordination polymer $[Co(bipy)_{1.5}(NO_3)_2]$. CS_2, a new motif for a network sustained by 'T-shape' building blocks. *New J. Chem.* **1998**, 177−181.

(20) Kepert, C. J.; Rosseinsky, M. J. Zeolite-like crystal structure of a microporous molecular framework. *Chem. Commun.* **1999**, 375−376.

(21) Cussen, E. J.; Claridge, J. B.; Kepert, C. J.; Rosseinsky, M. J. Flexible sorption and transformation behavior in a microporous metal-organic framework. *J. Am. Chem. Soc.* **2002**, *124*, 9574−9581.

(22) Losier, P.; Zaworotko, M. J. A noninterpenetrated molecular ladder with hydrophobic cavities, *Ang. Chem., Int. Ed. Engl.* **1996**, *35*, 2779−2782.

(23) Page, P. C. B.; Hutchings, G. J.; Bethell, D. Enantioselective heterogeneous catalysis using modified zeolite catalysts. *Chim. Oggi* **2001**, *19*, 14−17.

(24) Davis, M. E.; Lobo, R. F. Zeolite and Molecular-Sieve Synthesis. *Chem. Mater.* **1992**, *4*, 756−768.

(25) Ngo, H.; Lin, W. Chiral crown ether pillared lamellar lanthanide phosphonates. *J. Am. Chem. Soc.* **2002**, *124*, 14298−14299.

(26) Seo, J. S.; Whang, D.; Lee, H.; Jun, S. I.; Oh, J.; Jeon, Y. J.; Kim, K. A homochiral metal-organic porous material for enantioselective separation and catalysis. *Nature* **2000**, *404*, 982−986.

(27) Hu, A.; Ngo, H. L.; Lin, W. Chiral porous hybrid solids for practical heterogeneous asymmetric hydrogenation of aromatic ketones. *J. Am. Chem. Soc.* **2003**, *125*, 11490−11491.

(28) Robson, R.; Abrahams, B. F.; Moylan, M.; Orchard, S. D. Zinc saccharate: A robust, 3D coordination network with two types of isolated, parallel channels, one hydrophilic and the other hydrophobic. *Angew. Chem., Int. Ed.* **2003**, *42*, 1848−1851.

(29) Anokhina, E. V.; Jacobson, A. J. $[Ni_2O$(L-Asp)$(H_2O_2)\cdot 4H_2O$: A Homochiral 1D Helical Chain Hybrid Compound with Extended Ni−O−Ni Bonding. *J. Am. Chem. Soc* **2004**, *126*, 3044−3045.

(30) Gordon, L. E.; Harrison, W. T. A. Amino acid templating of inorganic networks: Synthesis and structure of L-asparagine zinc phosphite. *Inorg. Chem.* **2004**, *43*, 1808−1809.

(31) Guillou, N.; Livage, C.; Drillon, M.; Ferey, G. The chirality, porosity, and ferromagnetism of a 3D nickel glutarate with intersecting 20-membered ring channels. *Angew. Chem., Int. Ed.* **2003**, *42*, 5314−5317.

(32) Wells, A. F. *Three-Dimensional Nets and Polyhedra*; Wiley-Interscience: New York, 1977.

(33) Kepert, C. J.; Prior, T. J.; Rosseinsky, M. J. A versatile family of interconvertible microporous chiral molecular frameworks: The first example of ligand control of network chirality. *J. Am. Chem. Soc.* **2000**, *122*, 5158−5168.

(34) Prior, T. J.; Rosseinsky, M. J. Chiral direction and interconnection of helical three-connected networks in metal-organic frameworks. *Inorg. Chem.* **2003**, *42*, 1564−1575.

(35) Bradshaw, D.; Prior, T. J.; Cussen, E. J.; Claridge, J. B.; Rosseinsky, M. J. Permanent microporosity and enantioselective sorption in a chiral open framework. *J. Am. Chem. Soc.* **2004**, *126*, 6106−6114.

AR0401606